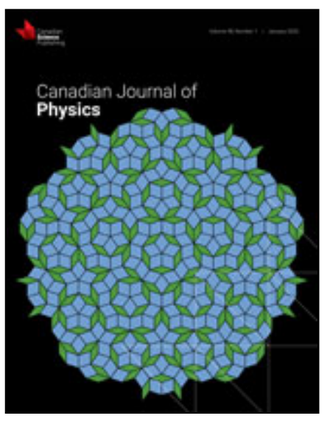

Browse the journal
- List of issues
- e-First articles
- Just-IN articles
- Current issue
- Special issues
- Most read articles
- Most cited articles
- Sample issue
- Author index

For authors
- About the journal
- Open Access
- Benefits and services
- Instructions to authors
- Submit a manuscript
- Permission forms
- Reprints & permissions to reuse content

Article « Previous TOC Next »

Calculations of Gamow-Teller Transition Strengths in some fp-Shell Nuclei using Shell Model

PDF (913 K)
PDF-Plus (936 K)

Fouad A. Majeed, Sarah M. Obaid

Published on the web 19 March 2020.
Received December 26, 2019.

Canadian Journal of Physics, https://doi.org/10.1139/cjp-2019-0693

ABSTRACT

The Gamow-Teller (GT) strength transitions in nuclear structure and astrophysical processes proved to be very important to understand the mechanisms of formation of neutron stars and black, therefore the Gamow-Teller (GT) transitions in the ⁴⁶Ti→⁴⁶V, ⁴⁷Ti →⁴⁷V ,⁴⁸Ti→⁴⁸V and ⁵⁰Cr→⁵⁰Mn charge-exchange reactions have been studied. The shell model calculations carried out in the fp- model space without any restriction using the GXFP1A, KB3G and FPD6 effective interactions. The calculation of the GT distribution is compared with the recent available experimental data. The theoretical calculations are in reasonably good agreement with the experimental GT distributions and with the summed transition strengths B(GT). For the individual transformations, we have reached a qualitative agreement while the measured cumulative transformation strengths are closely matched by the observed ones.

Calculations of Gamow-Teller Transition Strengths in some fp-Shell Nuclei using Shell Model

Fouad A. Majeed[1] and Sarah M. Obaid[2]

[1]Department of Physics, College of Education for Pure Sciences, University of Babylon, Babylon, Iraq.

[2]Department of Physics, College of Education for Pure Science (Ibn-Alhaitham), University of Baghdad, Baghdad, Iraq.

Abstract: The Gamow-Teller (GT) strength transitions in nuclear structure and astrophysical processes proved to be very important to understand the mechanisms of formation of neutron stars and black, therefore the Gamow-Teller (GT) transitions in the ^{46}Ti→^{46}V, ^{47}Ti →^{47}V ,^{48}Ti→^{48}V and ^{50}Cr→^{50}Mn charge-exchange reactions have been studied. The shell model calculations carried out in the fp- model space without any restriction using the GXFP1A, KB3G and FPD6 effective interactions. The calculation of the GT distribution is compared with the recent available experimental data. The theoretical calculations are in reasonably good agreement with the experimental GT distributions and with the summed transition strengths B(GT). For the individual transformations, we have reached a qualitative agreement while the measured cumulative transformation strengths are closely matched by the observed ones.

Keyword: Gamow-Teller transitions, Charge-exchange reactions, Isospin symmetry, Shell Model, Weak interaction

1. Introduction

Gamow-Teller (GT) strength transitions are the most common weak interaction processes of spin-isospin $(\sigma\tau)$ in atomic nuclei [1]. They are not only of particular interest to nuclear physics, but also to astrophysics; for example, they play an important role in the core failure of supernovae and nucleosynthesis type II [2,3]. Nonetheless, the direct research on the processes of weak decay provides relatively limited details of GT transitions and states excited by GT transfer (GT states). The β-decay can only be reached by the states with energies below the Q-value's decay. Nevertheless, beta decay has direct access to the half-live, Q_β values, and branching ratios analysis to the absolute GT transition strength B(GT). A simple operator $\sigma\tau$ causes the GT transitions and characterized by spin-isospin flip $(\Delta S = 1)$ and $(\Delta T = 1)$ and no transfer of angular momentum $(\Delta L = 0)$, as well as the z component of the isospin $T_z\left[T_z = (N - Z)/2\right]$ is changed by one unit $(\Delta T_z = \pm 1)$.

The reduced GT transition strength B(GT) is a significant physical quantity to study the nuclear structure. Typically, B(GT) levels are derived from GT decay studies. Furthermore, the intermediate energy reactions (>100 MeV/nucleon) of (p, n) or (^{3}He, t)

reactions can also be used to map out the GT strengths for a wide range of excitation energy (E_x) [1,4].

A systematic study was carried out by charge-exchange (CE) (n, p), (d,^{2}He) and (t,^{3}He) experiments on 13 based $45 \leq A \leq 64$ stable *fp*-shell nuclei by Cole and Anderson [5]. They argued that the CE rates derived from experimental B(GT) values are generally reproduced by shell model (SM) calculations satisfactorily, whereas QRPA calculations appear to overestimate experimental CE rates substantially.

Nuclear GT excitations for A = 42, 46,50, and 54 "fp-shell" nuclei for charge-exchange reactions (^{3}He, t) is reported by Fujita et al. in Ref. [6]. At 0° the incident energy is 140 MeV/nucleon and for the specific GT transition strengths B(GT) analysis, Adachi et al. conducted a high resolution (^{3}He, t) reaction from $T_z = +1$ (^{42}Ca, ^{56}Ti, ^{50}Cr and ^{54}Fe) to $T_z = 0$ (^{42}Sc, ^{46}V, ^{50}Mn and ^{54}Co) nuclei. The R^2 value, the ratio between the GT and Fermi cross-sections, was introduced to derive B(GT) values for these pf-shell nuclei. Numerous mass nuclei have been studied with the normal B(GT) value of β -decay studies and mass dependence has been extracted [7]. The nuclear Gamow-Teller (GT) transition strength distributions B(GT) have been studied by Obaid and Majeed [8], for some *sd*-shell nuclei in the (^{3}He, t) charge-exchange reaction. In their conducted study they employed the effective interactions USDA and USDB in the *sd*-model space and their results agree reasonably well with the measured data.

The residual interactions used with the modern shell model computations are updated libraries were developed for the *sd*-shell nuclei [9] and *fp*-shells for determination of the rates of weak-reactions [10,11]. The shell-model calculation was combined with experimental data, if available, to generate these libraries of weak-rate. Schemes outside the shell are necessary for nuclei beyond the pf-shell (see, e.g., [12]). Kumar and Srivastava [13] performed a systematic shell model calculation to describe the strengths of Gamow-Teller B(GT) and their accumulated sums for ^{42}Ti, ^{46}Cr, ^{50}Fe and ^{54}Ni nuclei. They had used GXPF1a and KB3G effective interactions in the full fp-model space to perform their calculations. Ganioğlu et al. [14] measured with high quality Gamow-Teller (GT) transitions for the transition $T_z = +3/2 \rightarrow +1/2$ transitions starting from the ^{47}Ti nucleus in the (3He,t) charge-exchange reaction at 0° and at an intermediate incident energy of 140 MeV/nucleon. They compared their measurements with shell model calculations using GXPF1 interaction which reproduce the experiment well. They found that the ratios of GT transition strengths to the ground state, the 0.088-MeV state, and the 0.146-MeV state are similar to the ratios of the strengths of the analogous M1 transitions from the isobaric analog state (IAS) to these states. Fujita et al. [15] studied the $T_z = -2 \rightarrow -1$ and $-1 \rightarrow 0$ GT transitions in decays, while those from stable $T_z = +2$ and +1 nuclei by means of hadronic (^{3}He, t) charge-exchange (CE) reactions. The results from these studies are compared in order to examine the mirror-symmetry structure in nuclei. In addition, these results are combined for the better understanding of GT transitions in the pf-shell region.

This work aims to calculate the GT strength distributions with higher excitation energies which is very useful for future experiments. The calculations of the GT strength distributions will be conducted in the framework of the shell model using NuShellX@MSU [16] to obtain the GT-strengths for ^{46}Ti$\rightarrow^{46}$V, ^{47}Ti $\rightarrow^{47}$V ,^{48}Ti$\rightarrow^{48}$V

and ^{50}Cr→^{50}Mn using GXFP1A [17], KB3G [18] and FPD6 [19] effective interactions in the full fp-model space. The results B(GT) values and their summed B(GT) will be compared with the corresponding experimental data.

2. Theoretical framework

The operator connecting the initial and the final states to the GT transition may be written as [20]

$$\langle \sigma\tau \rangle = \frac{\langle f \| \sum_k \sigma^k \tau_\pm^k \| i \rangle}{\sqrt{2J_i + 1}} \quad (1)$$

with

$$\tau_\pm = \frac{1}{2}(\tau_x + i\tau_y), \quad (2)$$

where σ is the operator of the Pauli and τ the isospin, $|i\rangle$ and $|f\rangle$, represents the initial and final transition states, respectively.

The B(GT) is the reduced probability of transition from GT, commonly used to indicate GT strength [20],

$$B(GT) = \left(\frac{g_A}{g_V}\right)^2 \langle \sigma\tau \rangle^2 \quad (3)$$

where $\left|g_A/g_V\right| = 1.26$, is the axial-vector ratio of constants to the vector coupling
The strength Gamow-Teller B(GT) is calculated using the following expression [21],

$$B(GT_\pm) = \frac{1}{2J_i + 1} f_q^2 \left| \left\langle f \left| \left| \sum_k \sigma^k \tau_\pm^k \right| \right| i \right\rangle \right|^2 \quad (4)$$

where f_q is the quenching factor, and the index k runs over the single particle orbitals, $|i\rangle$ and $|f\rangle$ describe the state of the parent and daughter nuclei, respectively.
. For reduced GT matrix elements, the sum rule is [21]

$$\sum_f [B_{i,f}(GT_-) - B_{i,f}(GT_+)] = 3\left(\frac{g_A}{g_V}\right)^2 (N_i - Z_i) \quad (5)$$

3. Results and Discussion

In this section, the theoretical results with the measured B(GT) strength transitions for ^{46}Ti→^{46}V, ^{47}Ti →^{47}V ,^{48}Ti→^{48}V and ^{50}Cr→^{50}Mn transitions. To obtain the B(GT)strength transitions we have carried out our theoretical calculations in the full *fp*-model space without any restriction, that is, assuming a ^{40}Ca inert core using the GXFP1A [17], KB3G [18] and FPD6 [19] effective interactions. The shell model calculations have been performed using NushellX@MSU and the results were compared to the corresponding measured data will be discussed for the selected *fp*-shell nuclei. All theoretical calculations for the three effective interactions are scaled by a quenching factor $(0.74)^2$ to agree with the measured data. The shell model calculations were performed in full *fp*-model space without any restriction imposed on the valence nucleons outside the ^{40}Ca core.

3.1 ^{46}Ti (^{3}He, t) ^{46}V

Figure 1 displays the measured and theoretical calculations of the shell model for B(GT) strengths transition from the ^{46}Ti (0^+) ground state to ^{46}V (1^+) states without any restriction using GXFP1A, KB3G and FPD6 effective interactions. The strength distribution of B(GT) has been measured in ^{46}Ti (^{3}He, t) experiment up to excitation energies below 4.5 MeV [22]. There are two dominant peaks from the experiment located at $E_x(^{46}V) = 0.994\ MeV\ and\ 2.978\ MeV$ with B(GT) values 0.365 and 0.604, respectively. These two peaks comes from the transitions $^{46}\mathrm{Ti}(0^+) \rightarrow {}^{46}\mathrm{V}(1_1^+)$ and ^{46}V(1_5^+) , respectively. The GXPF1A and KB3G interactions calculations showed one strong peak located at 2.628 MeV and 2.256 MeV with B(GT) values 1.148 and 1.031, respectively. This one peak in GXFP1A and KB3G interactions comes from the transition $^{46}\mathrm{Ti}(0^+) \rightarrow {}^{46}\mathrm{V}(1_3^+)$. The calculation of FPD6 interaction gives three peaks located at 0.0 MeV, 2.059 MeV and 2.414 MeV, with B(GT) values 0.539, 0.717 and 0.782, respectively. The rest of theoretical results are all below B(GT) value of 3 and they are in agreement with the observed experimental data.

The quenched shell model resulting from all interactions is capable of explaining the transition strength of GT observed concentrated at the energy of the lowest excitation.

Figure 2 shows the B(GT) running sum in terms of the excitation energy, the calculated strengths of the shell models in terms of the shell were calculated by a quenching factor $(0.74)^2$.The FPD6 interaction provided an energy of excitation closer to the measured data than the energy predicated by the GXPF1A and KB3G effective interactions.

The shell-model estimates some strength to be placed around 2.7 MeV excitation energy which is higher than the (^{3}He, t) observed data.

The strength of the summed B(GT) plot shown in Fig.2 indicates that the effective interaction with KB3G is closer to the experiment than effective interactions with GXPF1A and FPD6, the total strength of B(GT) predicted by GXPF1A combined with observed interactions better than with KB3G.

The summed B(GT) strengths in shell model agreed very well with the measured data. Many B(GT) values predicted by all interactions at $E_x \geq 4.5\ MeV$ MeV are not observed in the experiment, while the B(GT) values determined from shell model are similar to the experiment with higher excitation energies. Overall, the results of the shell model explained successfully the gross characteristics of the experimental B(GT) values as well as the summed B(GT) strengths.

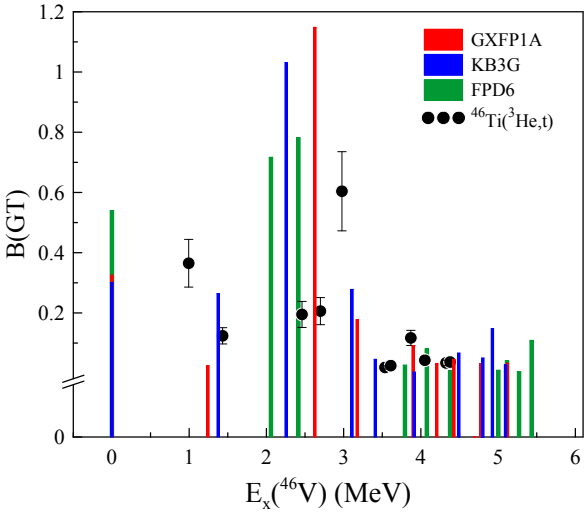

Figure 1: Shows the theoretical values of B(GT) compared to the corresponding experimental data [22] for ^{46}Ti $\rightarrow$^{46}V transition.

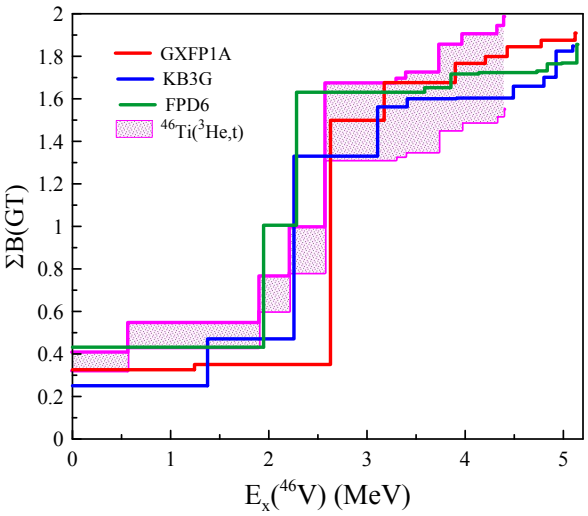

Figure 2: Shows the $\sum B(GT)$ distributions compared to measured data [22] for ^{46}Ti $\rightarrow$^{46}V transition.

3.2 ^{47}Ti (^{3}He, t) ^{47}V

Figure 3 displays a comparison between the calculations of the shell model using three interactions and the measured data for the transition ^{47}Ti$\rightarrow$^{47}V. The B(GT) transitions from ^{47}Ti (5/2$^-$) ground to (5/2$^-$) states can be found from a ^{47}V (^{3}He, t) experiment [19].

There are three dominated peaks from experiment located at $E_x(^{47}V) = 3.876\ MeV,\ 4.15\ MeV\ and\ 5.228\ MeV$ which came from the transition $^{47}\mathrm{Ti}\left(\frac{5}{2}^-_1\right) \rightarrow$ $^{47}\mathrm{V}\left(\frac{3}{2}^-, \frac{5}{2}^-, \frac{7}{2}^-\right)$ states with B(GT) values 0.112, 0.073 and 0.071, respectively. The rest of B(GT) values are weak strength less than 0.05. Shell model calculations of B(GT) using GXFP1A interaction predicted three peaks located at 0.67 MeV, 1.392 MeV and 1.512 MeV with B(GT) values 0.065, 0.105 and 0.086 MeV, respectively. The interaction KB3G calculation predicted two peaks located at 0.168 MeV and 1.96 MeV with B(GT) values 0.093 and 0.071, respectively. The calculation with FPD6 are in better agreement with experiment than GXFP1A and KB3G interactions.

The measured and calculated shell model strength distributions of B (GT) for the transition ^{47}Ti$\rightarrow$^{47}V. The B (GT) values ^{47}Ti (5/2$^-$) ground state to (5/2$^-$) states of ^{47}V (5/2$^-$) have been calculated without any truncation. The shell model calculations with KB3G interaction are more closely to the measured data than GXPF1A and FPD6 interactions.

Figure 4 displays the plot of the running sum of B(GT) as a function of excitation energy for the transition ^{47}Ti$\rightarrow$^{47}V.

The close similarity in strength of B(GT), predicted by the three interactions and (^{3}He, t) data, can be seen in the combined strength plot as shown in Fig.3.

The summed B(GT) strengths from KB3G interaction calculation is closely reproduced the measured data better than GXPF1A and FPD6 effective interactions.

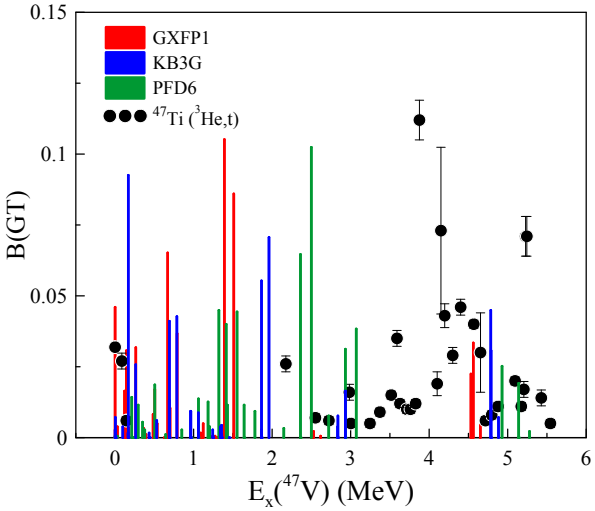

Figure 3: Shows the theoretical values of B(GT) compared to the corresponding experimental data [19] for ^{47}Ti→^{47}V transition.

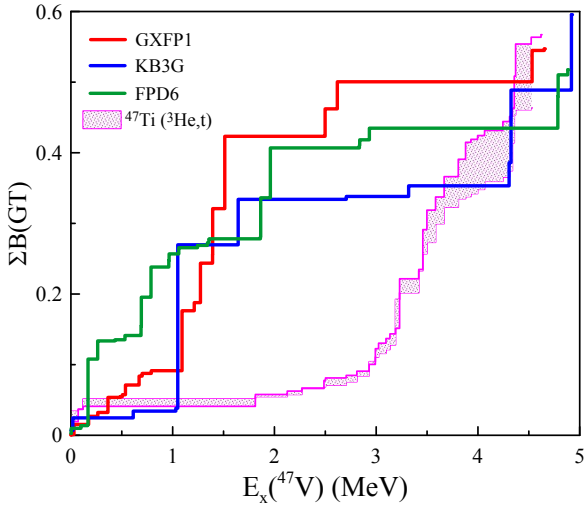

Figure 4: Shows the $\sum B(GT)$ distributions compared to the experimental data [19] for ^{47}Ti→^{47}V transition.

3.3 ^{48}Ti (^{3}He, t) ^{48}V

The calculations of the shell model and the GT strength distributions data are displayed in Fig.5 for the transition ^{48}Ti→^{48}V. The observed data through the reaction of charge-exchange ^{48}Ti(^{3}He, t)^{48}V up to the excitation energy $E_x(^{48}V) = 4.857 MeV$ [24] are shown in Fig. 5. The experimental data has three vales of B(GT) greater than 0.2 located at 0.421 MeV, 2.406 MeV and 3.864 MeV with B(GT) values 0.224, 0.351 and 0.213. The ground state for both ^{48}Ti and ^{48}V isotopes is predicted precisely by the three interactions. The interactions GXFP1A and KB3G predicts weak B(GT) values that agrees with the observed data, while the interaction FPD6 have strong dominated peak located at 2.796 MeV with B(GT) value 0.695 which is much higher than the values observed in the experiment.

Figure 5 shows that the strength of GT is highly fragmented and distributed in many discrete states, and that the shell model calculations have the same pattern using the three effective interactions. The experimental data observed from values comes from the The shell model calculations with FPD6 effective interactions overpredict the experimental data by amount of 0.4 MeV.

The best results achieved for the shell model calculations of B (GT) and their running sums is by using KB3G effective interaction.

The B (GT) strength distribution in ^{48}V is measured by ^{48}Ti (^{3}He, t) for transition from (0^{+}) ground state (1^{+}) states [23]. Figure 5 displays the theoretical calculations of strength distribution of GT by using effective interactions of GXFP1A, KB3G and FPD6. The running sums of B(GT) are shown in Fig.6 as a function of excitation energy for the transition ^{48}Ti→^{48}V.

The quenched shell model, which results from all interactions, is capable of explaining the observed GT transition strength distributed in most excited energies in ^{48}V.

The summed B(GT) strength figure shows that the shell model findings for the three adopted interactions match well with the summed strength of B(GT) observed and shows that in ^{48}Ti→^{48}V transition, this means that the fp-model space utilized without any truncation reproduce the data satisfactorily.

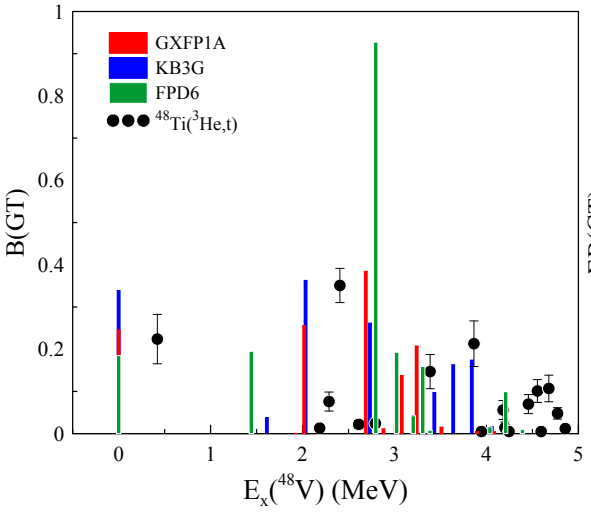

Figure 5: Shows the theoretical values of B(GT) compared to the corresponding experimental data [23] for ^{48}Ti →^{48}V transition.

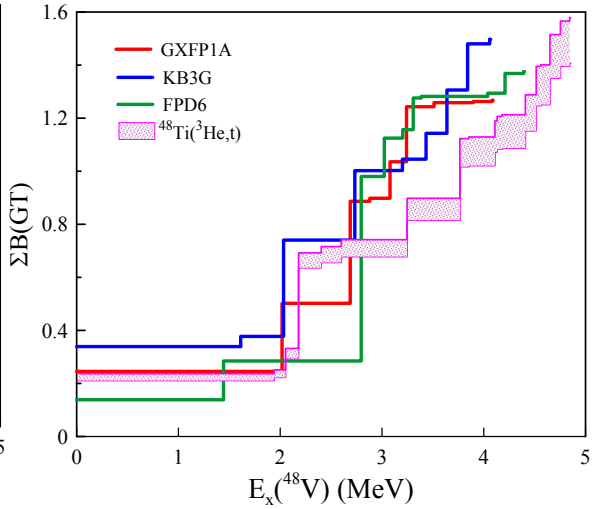

Figure 6: Shows the $\Sigma B(GT)$ distributions compared to the experiment for ^{48}Ti. The experimental data [23] for ^{48}Ti →^{48}V transition.

3.4 ^{50}Cr→^{50}Mn

The theoretical calculations of the shell model and the B(GT) data distribution strengths for the transition ^{50}Cr→^{50}Mn are displayed in Figure 7. The measured data observed through the reaction ^{50}Cr (^{3}He, t) ^{50}Mn up to excitation energy $E_x(^{50}Mn)$ =4.6MeV [21]. The calculations of the shell model in model space *fp* using the GXFP1A, KB3G and FPD6 effective interactions, respectively. There are two dominated peaks in the observed data located at $E_x(^{50}Mn)$ = 0.652 MeV and 3.392 MeV with B(GT) values 0.5 and 0.35, respectively. These two peaks came from the transitions ^{50}Cr(0^{+}) → ^{50}Mn(1_1^{+}) and ^{46}V(1_5^{+}), respectively. The shell model calculations with GXFP1A predicted two dominant

peaks located at 0.0 MeV and 2.377 MeV with B(GT) values 0.434 and 0.463, respectively. FPD6 interactions predict two strong peaks located at 0.0 MeV and 2.447 MeV with B(Gt) values 0.632 and 0.779, respectively. The calculation with KB3G is more consistent with the observed data than GXFP1A and FPD6.

The energies of the excited states for different 1^+ of ^{50}Mn are shown on the horizontal axis. In measured data, the strength of B(GT) is distributed over wide scale of ^{50}Mn excitation energies. We can see the peaks of most intensity at the excitation energies 0.652 MeV and 4.584 MeV of ^{50}Mn from experimental data for ^{50}Cr (^{3}He, t)^{50}Mn.

Figure 8 shows the B(GT) sum versus the excitation energy. The strength of B(GT) sums is displayed up to the excitation energy 1.4 MeV. The GXFP1A, KB3G and FPD6 interactions gives an appropriate measured data agreement especially in the region of high excitation energy above 2.5 MeV and the closer results is obtained by using KB3G interaction.

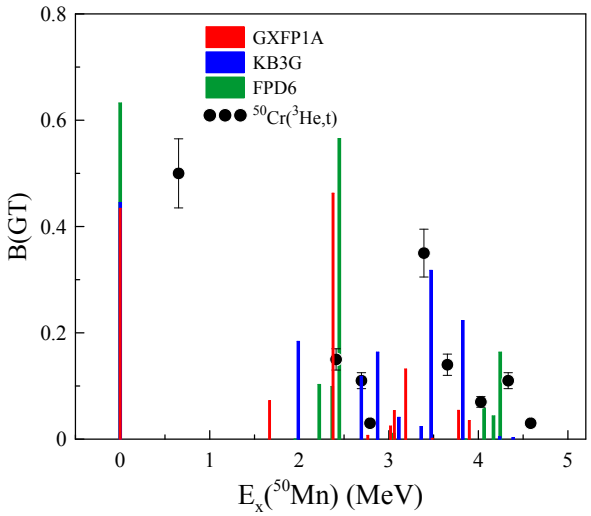

Figure 7: Shows the theoretical values of B(GT) compared to the corresponding experimental data [24] for ^{50}Cr→^{50}Mn transition.

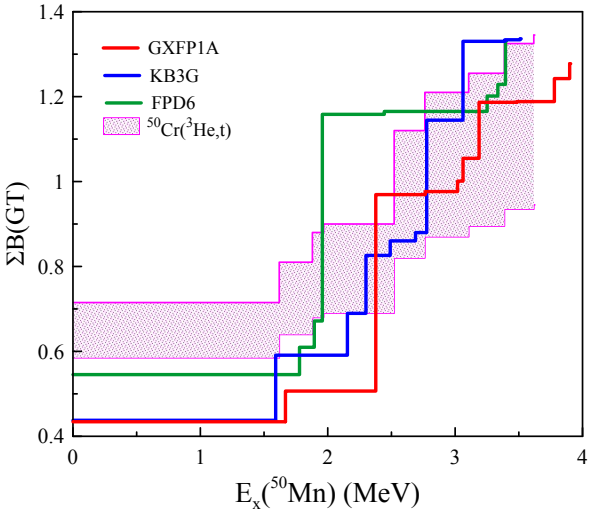

Figure 8: Shows the $\sum B(GT)$ distributions compared to the experiment [24] for ^{50}Cr →^{50}Mn transition.

4. Conclusion

In the present work we have reported the shell model calculations in the full fp-hell model space using GXFP1A, KB3G and FPD6 effective interactions without any truncation imposed on the valence nucleons to study the GT strengths of ^{46}Ti→^{46}V, ^{47}Ti →^{47}V ,^{48}Ti→^{48}V and ^{50}Cr→^{50}Mn transitions. For the individual B(GT) transitions, the qualitative agreement is achieved while the overview values measured are closely replicated. This study might give useful information to researchers who are interested to study the B(GT) transition strengths in this mass region. For these strengths, further

experimental results are needed. More information will be added to earlier works by the results of this work.

References

[1] F. Osterfeld, Nuclear spin and isospin excitations, Rev. Mod. Phys. 64 (1992) 491-557.

[2] K. Langanke and G. Martínez-Pinedo, Nuclear weak-interaction processes in stars, Rev. Mod. Phys. 75 (2003) 819-862.

[3] A. Heger, K. Langanke, G. Martínez-Pinedo, and S. E. Woosley, Presupernova Collapse Models with Improved Weak-Interaction Rates, Phys. Rev. Lett. 86 (2001) 1678-1681.

[4] J. Rapaport and E. Sugarbaker, Isovector excitations in nuclei, Annu. Rev. Nucl. Part. Sci. 44 (1994) 109-153.

[5] A. L. Cole, T. S. Anderson, R. G. T. Zegers, S. M. Austin, B. A. Brown, L. Valdez, S. Gupta, G. W. Hitt, and O. Fawwaz, Gamow-Teller strengths and electron-capture rates for pf-shell nuclei of relevance for late stellar evolution, Phys. Rev. C 86 (2012) 015809.

[6] Y. Fujita, H. Fujita,T. Adachi, C. L. Bai, A. Algora, G. P. A. Berg, P. von Brentano, G. Colò, M. Csatlós, J. M. Deaven, E. Estevez-Aguado, C. Fransen, D. De Frenne, K. Fujita, E. Ganioğlu, C. J. Guess, J. Gulyás,K. Hatanaka, K. Hirota, M. Honma, D. Ishikawa, E. Jacobs, A. Krasznahorkay, H. Matsubara, K. Matsuyanagi, R. Meharchand, F. Molina, K. Muto, K. Nakanishi, A. Negret, H. Okamura, H. J. Ong, T. Otsuka, N. Pietralla, G. Perdikakis, L. Popescu, Rubio,4 H. Sagawa, P. Sarriguren, C. Scholl,Y. Shimbara, Y. Shimizu, G. Susoy, T. Suzuki, Y. Tameshige, A. Tamii, J. H. Thies, M. Uchida, T.Wakasa, M. Yosoi, R. G. T. Zegers, K. O. Zell, J. Zenihiro. Observation of Low-and High-Energy Gamow-Teller Phonon Excitations in Nuclei, Phys. Rev. Lett. 112 (2014) 112502.

[7] T. Adachi et al., Gamow-Teller transitions in pf- shell nuclei studied in (^{3}He, t) reactions, Nucl. Phys. A 788 (2007) 70c–75c.

[8] S. M. Obaid and H. M. Tawfeek, Gamow-Teller strengths of some sd-shell nuclei in the shell model framework, submitted to Revista Mexicana de Física, (accepted).

[9] T. Oda, M. Hino, K. Muto, M. Takahara, K. Sato, Rate Tables for the Weak Processes of sd-Shell Nuclei in Stellar Matter, At. Data Nucl. Data Tables, 56 (1994) 231− 403.

[10] K. Langanke and G. Martínez-Pinedo, Shell-model calculations of stellar weak interaction rates: II. Weak rates for nuclei in the mass range A=45−65 in supernovae environments, Nucl. Phys. A. 673 (2000) 481-508.

[11] K. Langanke and G. Martínez-Pinedo, Rate tables for the weak processes of pf-shell in stellar environments, At. Data Nucl. Data Tables. 79 (2001) 1- 46.

[12] H.-T. Janka, K. Langanke, A. Marek, G. Martínez-Pinedo, and B. Müller, Theory of core-collapse supernovae, Phys. Rep. 442 (2007) 38-74.

[13] Vikas Kumar and P.C. Srivastava, Shell model description of Gamow-Teller strengths in pf-shell nuclei, Eur. Phys. J. A 52 (2016) 18: 1-8.

[14] E. Ganioğlu et al., High-resolution study of Gamow-Teller transitions in the ^{48}Ti (^{3}He, t)^{48}V reaction, Phys. Rev. C 93 (2016) 064326.

[15] Y. Fujita, B. Rubio, F. Molina, T. Adachi, H. Fujita, B. Blank, E. Ganigoğlu, W. Gelletly and S.E.A. Orrigo, Gamow-Teller transitions in pf-shell nuclei studied in (^{3}He, t) reactions, Act. Phys. Pol. B 47 (2016) 867-881.

[16] B. A. Brown, W. D. Rae, E. McDonald, M. Horoi, NuShellX@MSU, MSU-NSCL report C. 524 (2007) 1-29.

[17] M. Honma, T. Otsuka, B. A. Brown, and T. Mizusaki, Shell-model description of neutron-rich pf-shell nuclei with a new effective interaction GXPF1, Eur. Phys. Jour. A 25 (2005) 499-502.

[18] A. Poves, J. Sánchez-Solano, E. Caurier, F. Nowacki, Shell model study of the isobaric chains A=50, A=51 and A=52, Nucl. Phys. A. 694 (2001)157-198.

[19] W. A. Richter, M. G. Van Der Merwe, R. E. Julies, B. A. Brown, New effective interactions for the 0f1p shell, Nucl. Phys. A 523(1991) 325-353.

[20] W.-T. Chou, E. K. Warburton, and B. A. Brown, Gamow-Teller beta-decay rates for A≤18 nuclei, Phys. Rev. C 47 (1993) 163-177.

[21] Y. Fujita, B. Rubio, W. Gelletly, Spin–isospin excitations probed by strong, weak and electro-magnetic interactions, Prog. Part. Nucl. Phys. 66 (2011) 549-606.

[22] T. Adachi et al., High-resolution study of Gamow-Teller transitions from the T_z=1 nucleus^{46}Ti to the T_z=0nucleus^{46}V, Phys. Rev. C **73** (2006) 024311.

[23] E. Ganioğlu et al., High-resolution study of Gamow-Teller transitions in the ^{47}Ti (^{3}He, t)^{47}V reaction, Phys. Rev. C 87(2013) 014321.

[24] Y. Fujita et al., Gamow-Teller Strengths in Proton-Rich Exotic Nuclei Deduced in the Combined Analysis of Mirror Transitions, Phys. Rev. Lett. 95 (2005) 212501.